Asymmetric probability densities in symmetrically modulated bistable devices

M. Borromeo[1] and F. Marchesoni[2]
[1]*Dipartimento di Fisica, and Istituto Nazionale di Fisica Nucleare, Universitá di Perugia, I-06123 Perugia, Italy*
[2]*Dipartimento di Fisica, Universitá di Camerino, I-62032 Camerino, Italy*
(Received 16 July 2004; revised manuscript received 22 December 2004; published 21 March 2005)

A Brownian particle hopping in a symmetric double-well potential can be statistically confined into a single well by the simultaneous action of (a) two periodic input signals, one tilting the minima and the other one modulating the barrier height, and (b) an additive and a purely multiplicative random signal, generated by a unique source and thus preserving a certain degree of statistical correlation. The underlying gating mechanism is quite robust when compared, for instance, with biharmonic rocking. In view of technological implementation, asymmetric confinement through gating can be conveniently maximized by tuning the input signal parameters (correlation time, phase-time lag, amplitudes), thus revealing a resonant localization mechanism of general applicability.

DOI: 10.1103/PhysRevE.71.031105 PACS number(s): 05.40.−a, 02.50.Ey, 82.20.−w

I. INTRODUCTION

A Brownian particle bound by a bistable potential diffuses symmetrically between two potential minima; this is the case of Kramers' dynamics [1], where the particle is activated solely by thermal fluctuations, as well as of stochastic resonance (SR) [2], where the particle escape over the potential barrier is controlled by the interplay of noise and external periodic drive(s). In both cases the time-averaged particle distribution densities peak symmetrically in correspondence with the potential minima; particle localization into one well is customarily achieved by applying an external static bias that breaches the symmetry of the system [3].

For practical purposes experimenters are interested in confining the diffusing particle around one stable configuration and then manipulating it by means of various techniques; recent examples include magnetic flux microscopy [4], laser traps [5], quantum device design [6], and chemical reaction control [7], to mention but a few. However, in most circumstances adding an external bias to the system under study is inconvenient, hence the need for an alternate approach to the confinement problem.

In a recent paper we proved that confinement in a noisy bistable device may be achieved without apparent symmetry breaking [8]. A Brownian particle driven by a white, zero-mean Gaussian noise (mimicking thermal fluctuations) and, possibly, by a sinusoidal force with angular frequency Ω_1 can be localized into one state by modulating the potential barrier separating the two degenerate states. To this purpose one can either input a sinusoidal control signal with frequency Ω_2 or recycle the additive noise back through a noisy transmission line with time delay τ_d and residual correlation λ. In both schemes the corresponding steady distribution densities develop one prominent peak, whose relative magnitude hits a *resonance* maximum (of over 95%) for optimal values of the input parameters (Ω_1 and Ω_2 or τ_d and λ, respectively); which degenerate state the particle gets trapped in depends on the switch-on phase of the modulating signal.

The present article is organized as follows. In Sec. II we introduce a simple model of periodically rocked-pulsated double well; the overdamped stochastic dynamics that takes place over the modulated barrier is gated toward one preferred well, depending on the relative phase of the applied drives. In Sec. III we compare this instance of asymmetric confinement with an even simpler but less robust example, where asymmetry is obtained through a biharmonic drive, an indirect manifestation of harmonic mixing. In Sec. IV we show that the gating mechanism of Sec. II can be generalized to the case of noisy modulating drives with appropriate statistical cross correlation and/or relative time delay.

II. ROCKED-PULSATED DOUBLE WELL

The key mechanism underlying the phenomenon of asymmetric confinement is well illustrated by the study model of an overdamped Brownian particle of coordinate $x(t)$ diffusing in a quartic double-well potential $V(x)=-ax^2/2+bx^4/4$, with $a,b>0$, subjected to a zero-mean Gaussian noise $\xi(t)$ and two rectangular signals $\epsilon_i(t)=\epsilon_i \,\mathrm{sgn}[\cos(\Omega_i t+\phi_i)]$, $i=1,2$, with periods $T_i=2\pi/\Omega_i$—namely,

$$\dot{x}=a[1+\epsilon_2(t)]x-bx^3+ax_0\epsilon_1(t)+\xi(t) \qquad (1)$$

and $\langle \xi(t)\xi(0)\rangle=2D\delta(t)$. Here, the additive signal $\epsilon_1(t)$ rocks the potential sidewise, whereas the control signal $\epsilon_2(t)$ sets the symmetric barrier separating the degenerate minima $\pm x_0=\pm\sqrt{a/b}$, to a high-low height $\Delta V_\pm=\Delta V_0(1\pm\epsilon_2)^2$, with $\Delta V_0=a^2/4b$. The two configurations of the rocked-pulsated potential are shown in Fig. 1.

The steady (time-averaged) distribution densities $P(x)$ of the stochastic process (1) have been computed by standard numerical simulation. In Fig. 2(a) our numerical data for $\Omega_1=\Omega_2$ and $\phi_1=\phi_2=0$ exhibit a marked asymmetry, corresponding to a stochastic confinement of the particle to the left-hand side (LHS)—i.e., in the negative potential well. In view of the input signal synchronization, a qualitative interpretation of this outcome is immediate: As long as the driving force $\epsilon_1(t)$ points to the right, the barrier is set to its larger value ΔV_+, so that the Brownian particle takes a relatively long time to jump into the more stable well to the right (from where it can hardly escape); vice versa, as the additive

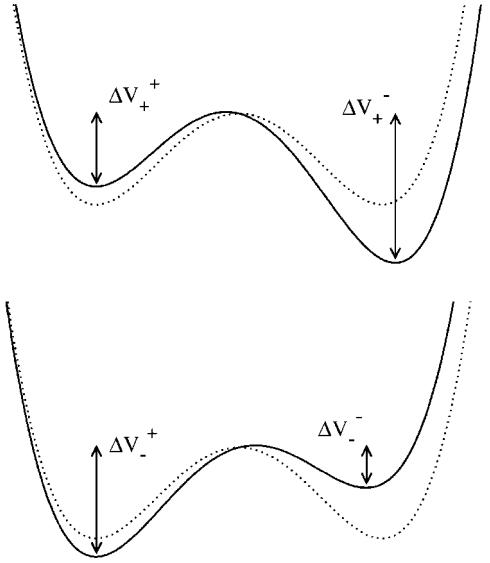

FIG. 1. Rocked-pulsated quartic double-well potential (1): $a=b=1$, $\epsilon_1=\epsilon_2=0.1$. The two configurations for $\epsilon_{1,2}(t)>0$ (upper) and $\epsilon_{1,2}(t)<0$ (lower) are contrasted with the unperturbed potential $V(x)$ (pointed curve). The relevant barrier heights are $\Delta V_-^-=0.111$, $\Delta V_+^+=0.2$, $\Delta V_-^+=0.3$, and $\Delta V_+^-=0.409$ (see text).

force reverses sign, the barrier switches to its lower value ΔV_-, thus speeding up the right-to-left escape process. As a result, the spatial distribution density $P(x)$ tends to accumulate around $-x_0$. Of course, shifting the relative phase $\phi_2-\phi_1$ by π is equivalent to changing $x\to -x$ and thus reversing asymmetry, as shown in Fig. 2(a).

The *gating* mechanism [9] invoked here is expected to become increasingly efficient as D is lowered below ΔV_0. In Fig. 2(b) the subtracted asymmetry factor $\sigma\equiv P_-/P_+-1$, with $P_\pm\equiv\langle\int_0^\infty P(\pm x,t)dx\rangle_t$ and $\langle\cdots\rangle_t$ denoting the stationary time average taken over one forcing cycle, diverges exponentially for $D\to 0$ and tends to zero (no confinement) according to a power law for $D\to\infty$.

The dependence of σ on the forcing period T_Ω, with $T_\Omega=T_1=T_2$ (*synchronous* signals), reveals a broad resonance peak [Fig. 2(c)]. This property points to an underlying resonant activation mechanism [10]: Due to the rectangular modulation $\epsilon_2(t)$, the bistable potential switches between two configurations $V_\pm(x)=-a(1\pm\epsilon_2)x^2/2+bx^4/4$; the two-valued tilting term $\mp\epsilon_1 a x_0 x$ removes the symmetry of the corresponding barriers $\Delta V_\pm$—that is, when jumping to the right (left), the particle overcomes different tilted barriers with heights $\Delta V_\pm^+$ ($\Delta V_\pm^-$), respectively. For the kind of $\epsilon_{1,2}(t)$ signals employed here—i.e., in-phase and of comparable amplitudes $0<\epsilon_1\sim\epsilon_2\ll 1$—these four barrier heights obey the inequalities $\Delta V_-^-\ll\Delta V_+^+\lesssim\Delta V_-^+\ll\Delta V_+^-$ (see Fig. 1). As anticipated above, the direct (left-to-right) escape time T_+^+ over the higher barrier ΔV_+ is much larger than the reverse escape time T_-^- over the lower barrier ΔV_-, thus causing an accumulation of the probability density in the negative well. However, when the forcing period T_Ω grows much longer than T_-^-, probability leakage through direct escape over both barrier configurations starts degrading the gating effect, so that P_-/P_+ decays back *close* to unity.

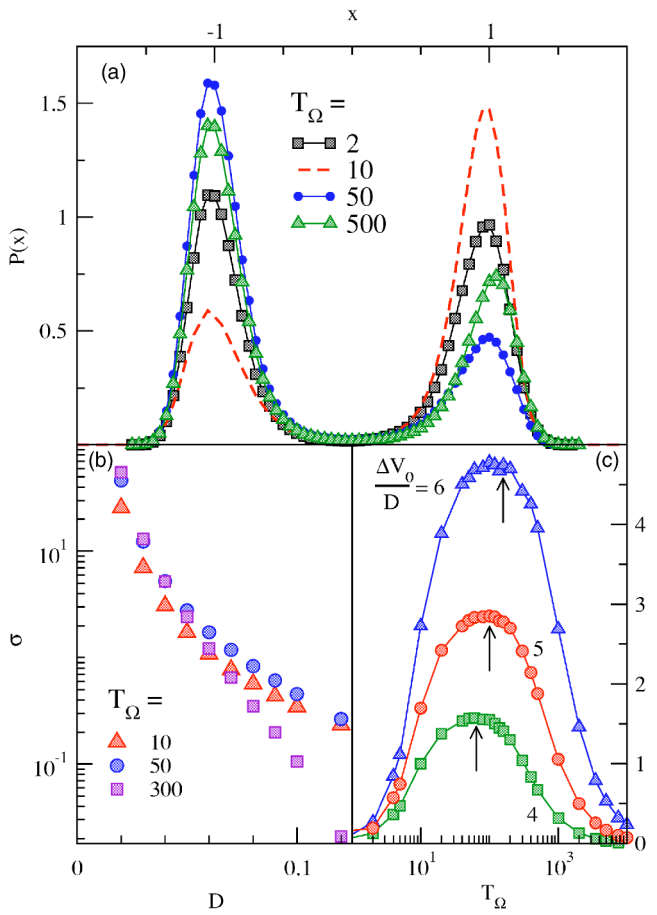

FIG. 2. (Color online) (a) Time-averaged probability densities $P(x)$ of the process (1) for different periods $T_1=T_2=T_\Omega$. Simulation parameters: $\epsilon_1=\epsilon_2=0.1$, $a=b=1$, $\Delta V_0/D=4$, $\phi_2-\phi_1=\pi$ (dashed curve) and $\phi_2-\phi_1=0$ (all remaining curves); see Fig. 1. Time averages are taken over 10^5 cycles. (b) Subtracted asymmetry σ versus D for $\phi_2-\phi_1=0$ and three different values of T_Ω; (c) σ versus T_Ω for $\phi_2-\phi_1=0$ and three different values of $\Delta V_0/D$. A vertical arrow marks $T_\Omega=2T_-^-$, T_-^- being the corresponding shortest Kramers' escape time.

The dynamics of confinement under the conditions of Fig. 2 is further illustrated in Fig. 3(a), where the distributions of the escape times T from the left to the right, $N_+(T)$, and vice versa, $N_-(T)$, are plotted for an optimal choice of the modulation period—i.e., $T_\Omega\sim T_-^-/2$. As expected [11], escape times equal to odd multiples of $T_\Omega/2$ are favored in both directions; however, only the reverse (right-to-left) escape process is closely synchronized with the in-phase periodic signals $\epsilon_1(t)$ and $\epsilon_2(t)$, as manifested by the prominent peak of $N_-(T)$ at $T=T_\Omega/2$. The escape phase analysis [13] in Fig. 3(b) clearly reveals the nonstationary nature of stochastic confinement: Under resonant conditions most jumps in either direction occur within one half forcing period from the latest switch of the two in-phase signals, with the synchronized jumps to the left outnumbering the synchronized jumps to the right.

In a more general setup, $\epsilon_1(t)$ and $\epsilon_2(t)$ may differ either in *phase*—for instance, when an external force acting upon the diffusing particle $x(t)$ also modulates its substrate $V(x)$

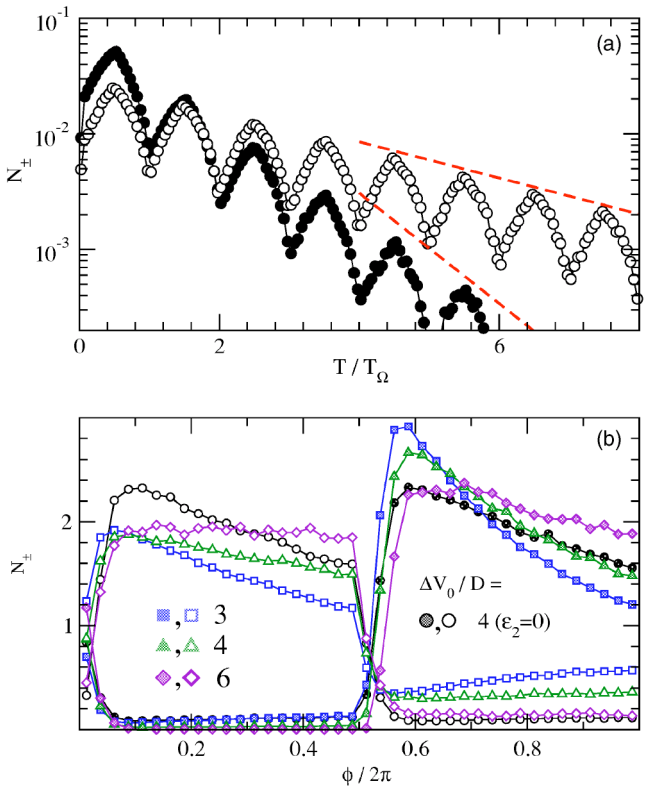

FIG. 3. (Color online) (a) Escape time distributions: left to right, $N_+(T)$ (solid symbols), and right to left, $N_-(T)$ (open symbols), for $\Delta V_0/D=4$, $T_\Omega=80$, and $\phi_2-\phi_1=0$. The other simulation parameters are as in Fig. 2(a). Note that the envelope (dashed) curves decay like $\exp(-T/T_\pm^*)$ with $T_\pm^*=2T_+^\pm T_-^\pm/(T_+^\pm+T_-^\pm)$ computed by means of Eq. (5.112) of Ref. [3]. (b) Escape phase distributions for different values of $\Delta V_0/D$, $T_\Omega=80$, and $\phi_2-\phi_1=0$: left to right (solid symbols) and right to left (open symbols). The escape phase $\phi/2\pi$ is defined as the time delay (in units of T_Ω) between a given in-phase $\epsilon_{1,2}(t)$ switch and the next particle jump. Solid and open circles represent the overlapping $N_\pm(T)$ distributions in the absence of barrier modulation—i.e., $\epsilon_2=0$.

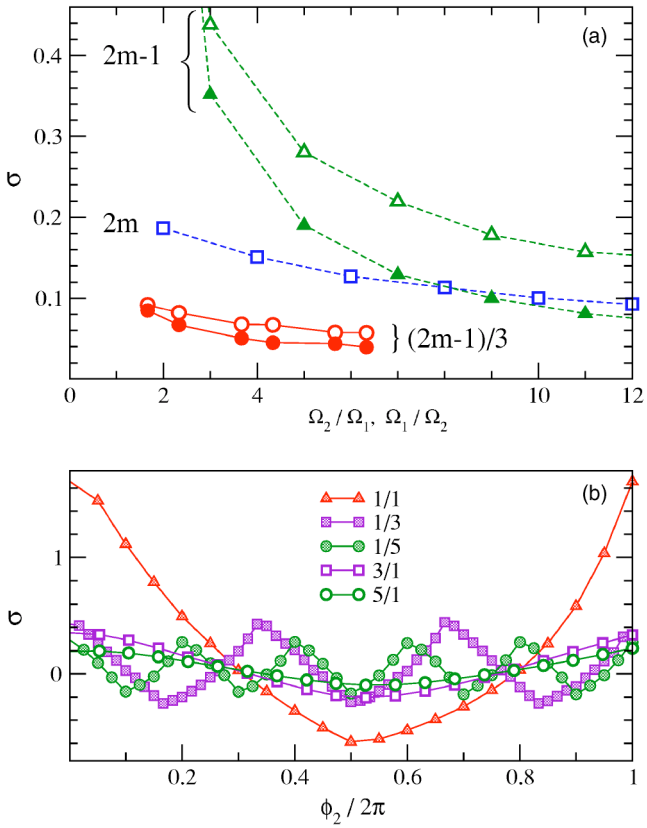

FIG. 4. (Color online) (a) Subtracted symmetry factor σ versus Ω_1/Ω_2 (open symbols) and Ω_2/Ω_1 (solid symbols) for $T_1=80$. Here, $\Delta V_0/D=4$ and $\phi_2-\phi_1=0$; the remaining simulation parameters are as in Fig. 2(a). Dashed curves connect the spikes belonging to the same family (with index shown). (b) σ versus ϕ_2 with $\phi_1=0$ and different values of Ω_1/Ω_2. All other simulation parameters are as in (a). Note that the oscillations displayed are well reproduced by the modulation factor $p(\Delta_{p,q})$ (see text).

with a phase lag that depends on the internal friction of the system [14]—or in *frequency*—corresponding to the case of two distinct input signals (say, a drive and a control signal). In Fig. 4(a) we plotted the subtracted asymmetry σ versus Ω_2 for fixed T_1 and $\phi_1=\phi_2$. A few remarkable properties are apparent: (i) Confinement occurs only for *commensurate* Ω_1 and Ω_2—namely, for $\Omega_1/\Omega_2=p/q$, with p,q prime integers. (ii) For irrational Ω_1/Ω_2 ratios, $P_-/P_+=1$ within numerical accuracy. (iii) The spikes of P_-/P_+ versus Ω_1/Ω_2 can be rearranged in families with "odd" indices $\Omega_1/\Omega_2=(2m-1)/(2n-1)$ or "even" indices $\Omega_1/\Omega_2=(2m-2)/(2n-1)$; both indices are obtained by keeping the integer n fixed and letting m run from $n+1$ to infinity (with the additional condition that numerators and denominators are prime integers)—i.e., $\Omega_1/\Omega_2>1$. Moreover, to each such Ω_1/Ω_2 family we can associate a family with identical "conjugate index" Ω_2/Ω_1. (iv) The smaller n, the more prominent is the spike family; moreover, within each family the spike amplitudes decrease with the running index m.

The efficiency of stochastic confinement depends on the phases of both signals: σ plotted versus ϕ_2 [Fig. 4(b)] oscillates around its average value 0 with amplitude proportional to the modulation factor $p(\Delta_{p,q})=|\pi-\Delta_{p,q}|/\pi-0.5$ (mod 1), where for $\Omega_1/\Omega_2=p/q$ the dephasing angle $\Delta_{p,q}$ reads $\Delta_{p,q}=p\phi_2-q\phi_1$.

The adiabatic limit $T_{1,2}\to\infty$, far from providing an optimal confinement, still allows a quantitative interpretation of the (out-of-resonance) properties listed above. For rectangular $\epsilon_{1,2}(t)$ input signals, the high-low barrier potentials $V_\pm(x)$ are tilted symmetrically to the right or left as $V_\pm^\pm(x)=V_\pm(x)\mp\epsilon_1 a x_0 x$. Correspondingly, if both forcing periods $T_{1,2}$ are much longer than the slowest escape time, then the time-averaged distribution density reads

$$P(x)=P_0(x)-(-1)^{m+n}\frac{\Delta_P(x)p(\Delta_{2m-1,2n-1})}{(2m-1)(2n-1)}, \qquad (2)$$

for $\Omega_1/\Omega_2=(2m-1)/(2n-1)$ and $P(x)=P_0(x)$ otherwise; here,

$$P_0(x) = \frac{1}{2}[P_+(x) + P_-(x)], \quad \Delta_P(x) = \frac{1}{2}[Q_+(x) - Q_-(x)], \tag{3}$$

where $P_\pm(x) = [e^{-V_\pm^+(x)/D} + e^{-V_\pm^-(x)/D}]/2N_\pm$ are even x functions, $Q_\pm(x) = [e^{-V_\pm^+(x)/D} - e^{-V_\pm^-(x)/D}]/2N_\pm$ are odd x functions, and $N_\pm = \int_{-\infty}^{\infty} e^{-V_\pm^+(x)/D} dx$ are suitable normalization constants. One notices immediately that in the adiabatic limit no P_-/P_+ spike is predicted for $\Omega_1/\Omega_2 = (2m-2)/(2n-1)$, consistently with the result of Fig. 4(a) that for finite $\Omega_{1,2}$ the even spikes with index $(2m-2)/(2n-1)$ are suppressed with respect to the corresponding odd spikes with index $(2m-1)/(2n-1)$. Moreover, in view of Eqs. (2) and (3), the amplitudes of the odd spike families decrease with the running index m towards the asymptotic value $P_-/P_+ \to (1+\delta)/(1-\delta) > 1$, with $\delta = \int_{-\infty}^{\infty} |\Delta_P(x)| dx/[(2m-1)(2n-1)]$ diverging exponentially for $D \to 0$ and tending to zero according to a power law for $D \to \infty$ [see Fig. 2(b)].

III. BIHARMONICALLY ROCKED DOUBLE WELL

The asymmetry of the time-averaged probabilities $P(x)$ in a modulated bistable system can always be traced back to some inherent asymmetry of the driving mechanism. In the gating effect of Sec. II such an asymmetry is due to the relative phase $\Delta_{p,q}$ of the input signals being kept constant throughout the process; the sign of a single signal cannot be reversed without changing $\Delta_{p,q}$.

This phenomenon has been overlooked even in the SR literature [2,12,15]. The most elementary model exhibiting asymmetric confinement we could think of corresponds to a simplified version of Eq. (1),

$$\dot{x} = ax - bx^3 + ax_0 F(t) + \xi(t), \tag{4}$$

where $\xi(t)$ is defined as above and

$$F(t) = A_1 \cos(\Omega_1 t + \phi_1) + A_2 \cos(\Omega_2 t + \phi_2). \tag{5}$$

Here, for commensurate frequencies $\Omega_1/\Omega_2 = p/q$, the biharmonic signal $F(t)$ is clearly asymmetric; the dynamics (4) is symmetric under signal reversal $F \to -F$ only for irrational Ω_1/Ω_2 [see inset in Fig. 5(b)].

No surprise that the time-averaged probability densities of the process (4) develop a certain degree of asymmetry, quantified by a nonzero factor σ (Fig. 5). However, determining the sign of σ is not as straighforward as in Sec. II.

In the adiabatic limit of Fig. 5, $\Omega_1, \Omega_2 \to 0$ with $\Omega_2/\Omega_1 = 2$ and $\phi_1 = \phi_2$, the zero-mean periodic drive $F(t)$ is negative during a larger fraction of its period T_1 than it is positive. As a consequence, one might predict an accumulation of the particle distributions in the negative well—that is, $\sigma > 0$. This is confirmed by the adiabatic estimate

$$P(x) = \langle P(x,t) \rangle_t, \tag{6}$$

with $P(x,t) = N(t)\exp[-V(x,t)/D]$, $V(x,t) = V(x) - ax_0 x F(t)$, and $\int_{-\infty}^{\infty} P(x,t) dx \equiv 1$; the resulting asymmetry factor attains a positive maximum for vanishingly low commensurate frequencies, in agreement with our numerical simulation [see Fig. 5(b)].

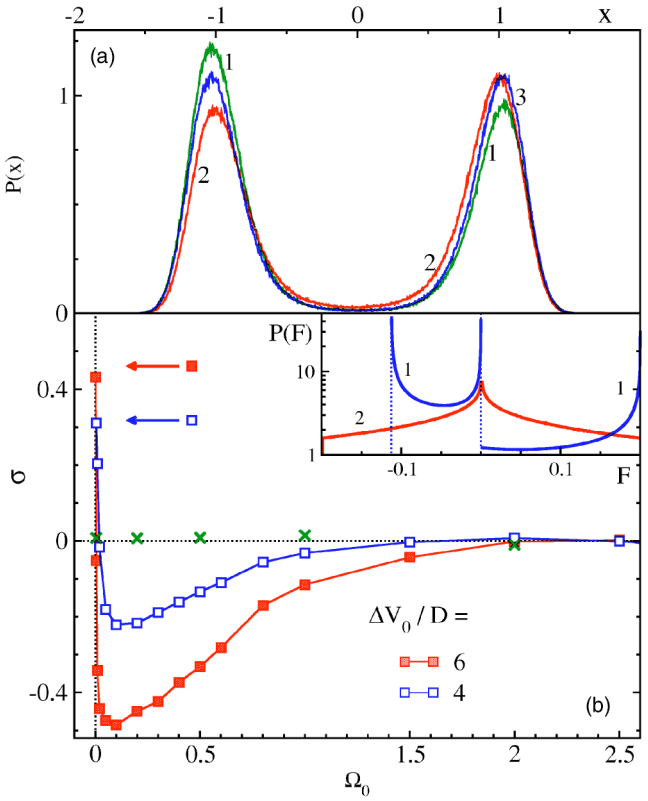

FIG. 5. (Color online) Biharmonically rocked double-well potential (4) and (5): (a) Time-averaged probability densities $P(x)$ of the process (4) for $\Delta V_0/D = 4$, and $\Omega_1 = 0.005$ and $\Omega_2 = 0.01$ (curve 1, green), $\Omega_1 = 0.1$ and $\Omega_2 = 0.2$ (curve 2, red), and $\Omega_1 = 0.1$ and $\Omega_2 = 0.1 \times \sqrt{5}$ (curve 3, blue). (b) Subtracted asymmetry σ versus $\Omega_1 \equiv \Omega_0$; blue open squares: $\Omega_2 = 2\Omega_0$ and $\Delta V_0/D = 4$; red solid squares: $\Omega_2 = 2\Omega_0$ and $\Delta V_0/D = 6$; green crosses: $\Omega_2 = \sqrt{5}\Omega_0$ and $\Delta V_0/D = 4$. Horizontal arrows point to the analytic estimate (6) for $\Omega_2 = 2\Omega_1 \to 0$ (same color code). Inset: distribution of the simulation forcing signal (5) sampled with time step 0.001: blue curve 1: $\Omega_2 = 2\Omega_1$ (asymmetric, commensurate case); red curve 2: $\Omega_2 = \sqrt{5}\Omega_0$ (symmetric, incommensurate case). Other simulation parameters: $a = b = 1$, $A_2 = A_1 = 0.1$, and integration time step 0.001.

Furthermore, numerical simulation shows that on increasing Ω_1 with $\Omega_2/\Omega_1 = 2$, σ decreases and eventually changes sign. This is an instance of the phenomenon known as resonant activation [10,16]. For $\phi_1 = \phi_2$ the forcing wave form (5) develops large-amplitude crests of relatively short time duration: as long as the forcing period T_1 is larger than T_+^+, but shorter than T_-^- (note here that $T_+^+ < T_-^+ < T_-^- < T_+^-$), the particle flow from left to right is favored and σ grows negative. For extremely fast oscillations of $F(t)$ the Brownian particle sees an average potential $\langle V(x,t) \rangle_t = V(x)$; i.e., no asymmetry effects are detectable. This is the behavior displayed by the curves σ versus Ω_1 in Fig. 5(b).

The process (4) exhibits asymmetric confinement as a result of the nonlinear combination of the two harmonic components of $F(t)$. Such a mechanism, experimentally established as *harmonic mixing*, was not much explored in the context of transport theory, until very recently [9]. However, at variance with harmonic mixing in a sinusoidal potential [17], here the induced probability unbalance changes sign

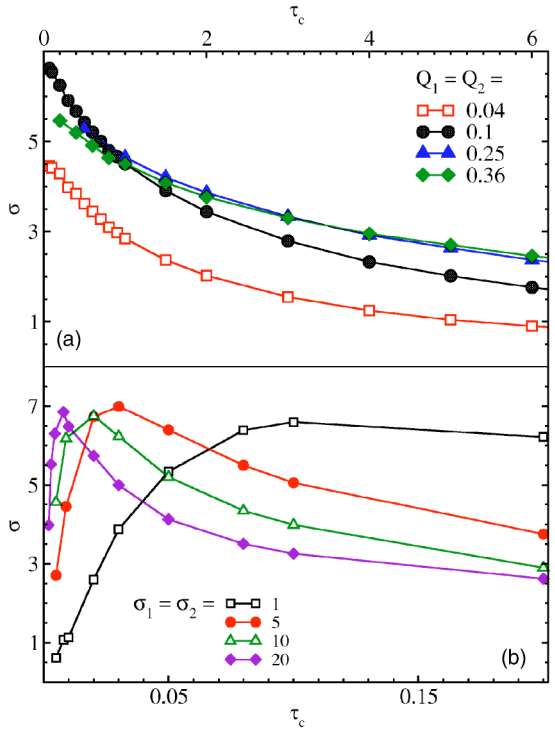

FIG. 6. (Color online) Noise mixing (1), (7): Subtracted asymmetry σ versus τ_c for different values of $Q_1=Q_2$ (a) and of the standard deviation $\sigma_1=\sigma_2$ (b); here $\sigma_i^2 \equiv Q_i/\tau_c$ (see text). Other simulation parameters: $a=b=1$, $\Delta V_0/D=4$, $\lambda=1$, and integration time step 0.001.

with Ω_1 (for Ω_1/Ω_2 a constant rational number), thus making this effect less robust and predictable than the gating effect of Sec. II.

IV. NOISE MIXING

We now come back to the focus of this paper—namely, to asymmetric confinement through gating. A variation of the mechanism under study can be achieved by employing two *correlated* noisy signals [18]. Let us consider the case of Eq. (1) when $\epsilon_{1,2}(t)$ denote two stationary, zero-mean-valued Gaussian noises with correlation functions

$$\langle \epsilon_i(t)\epsilon_j(0)\rangle = \lambda_{ij}\frac{\sqrt{Q_iQ_j}}{\tau_{ij}}\exp\left(-\frac{|t|}{\tau_{ij}}\right) \qquad (7)$$

and $\langle \xi(t)\epsilon_i(0)\rangle = 0$ $(i,j=1,2)$. To avoid technical complications we assume that $\tau_{ij}\equiv\tau_c$ and $\lambda_{11}=\lambda_{22}=1$. The parameter $\lambda\equiv\lambda_{12}=\lambda_{21}$ characterizes the two-signal cross correlation: namely, $\lambda=0$, independent signals; $\lambda=1$, identical signals, $\epsilon_2(t)\equiv\epsilon_1(t)$; $\lambda=-1$, signals with reversed sign, $\epsilon_2(t)\equiv-\epsilon_1(t)$. Two signals generated by a unique noise source can get partially decorrelated, $|\lambda|<1$, as an effect of different transmission or coupling mechanisms.

In the white noise limit $\tau_c\to 0$, the Fokker-Planck equation associated with the process (1), (7) admits of a stationary solution in closed form [19]—i.e.,

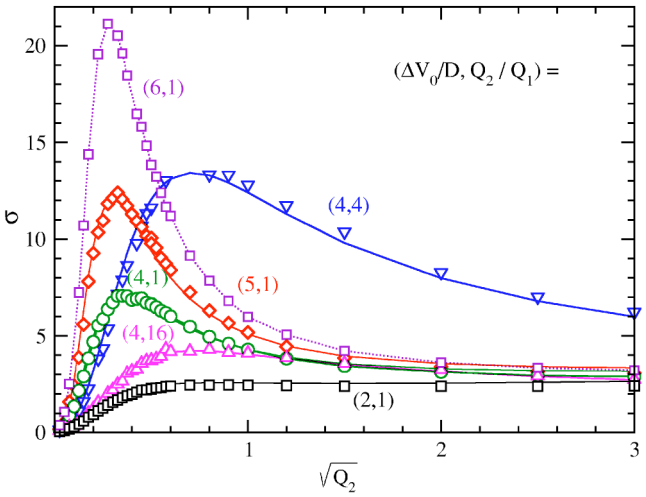

FIG. 7. (Color online) Noise mixing (1), (7): Subtracted asymmetry σ versus the intensity Q_2 of the *noisy* signal ϵ_2 for $\tau_c=0.005$ and different $\Delta V_0/D$ and Q_2/Q_1 (symbols, different colors); the corresponding analytical predictions for $\tau_c=0$, Eq. (8), are displayed as solid curves (same color). Other simulation parameters: $a=b=1$, $\lambda=1$, and integration time step 0.001. Note that setting $\lambda=1$ does not imply full statistical cross correlation between the multiplicative signal $\epsilon_2(t)$ and the total additive noise $\epsilon_1(t)+\xi(t)$.

$$P(x) = \frac{N}{[Q(x)+D]^{1/2}}\exp\left[-\int^x \frac{V'(y)dy}{Q(y)+D}\right], \qquad (8)$$

with $Q(x)=a^2(x_0^2Q_1+x^2Q_2+2\lambda x_0 x\sqrt{Q_1Q_2})$ and N a suitable normalization constant. The distribution $P(x)$ is clearly asymmetric for $\lambda\neq 0$ (see Figs. 6 and 7). Moreover, the sign of λ, similarly to the relative phase $\Delta_{m,n}$ in the ac case of Fig. 4(b), determines the well where the particle tends to localize.

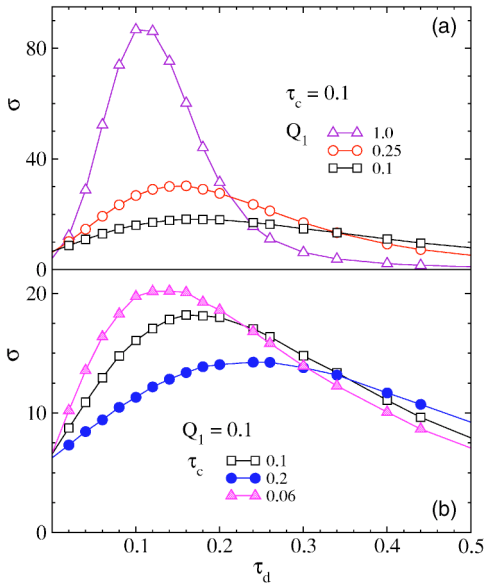

FIG. 8. (Color online) Subtracted asymmetry σ versus the relative ϵ_1, ϵ_2 delay time τ_d for different values of Q_1 (a) and τ_c (b). Other simulation parameters: $a=b=1$, $\Delta V_0/D=4$, $\lambda=1$, $Q_1=Q_2$, and integration time step 0.001.

The magnitude of the confinement effect is controlled by (i) the correlation time τ_c (Fig. 6). The subtracted asymmetry σ decays *exponentially* with τ_c from the corresponding analytic value of Fig. 7 down to the adiabatic estimate obtained by computing $\sigma=\sigma(\epsilon_1,\epsilon_2)$ at fixed ϵ_1,ϵ_2 and then averaging over the Gaussian distributions of ϵ_1,ϵ_2, $\sigma(\tau_c\to\infty)=\langle\sigma(\epsilon_1,\epsilon_2)\rangle_{1,2}$. The decay constant τ_c^* of the curves $\sigma=\sigma(\tau_c)$ is comparable with the adiabatic estimate $\langle T(\epsilon_1,\epsilon_2)\rangle_{1,2}$ of the relevant escape time $T(\epsilon_1,\epsilon_2)$ out of a deformed potential well. (ii) The additive noise intensities Q_1 and D (Fig. 7). For $\tau_c\to 0$ the analytical estimate of σ based on Eq. (8) reproduces quite closely our simulation results for $a\tau_c=0.005$ or smaller. For fixed Q_2 and D, the curves $\sigma(Q_1)$ *resonate* at a certain intensity of the *correlated* additive noise $\epsilon_1(t)$, whereas the asymmetry increases uniformly with decreasing the intensity D of the uncorrelated noise $\xi(t)$. Moreover, for large Q_2 the curves $\sigma(Q_2)$ approach an asymptotic value depending on D and Q_1 (also an adiabatic limit [10,16]).

A closer resemblance with the resonant dynamics underlying the ac confinement of Fig. 2 was obtained by assuming that ϵ_2 is transmitted with a *time delay* τ_d relative to ϵ_1—e.g., by replacing $\epsilon_2(t)\to\epsilon_2(t-\tau_d)$ in Eq. (1) [20]. In Fig. 8 the resonant nature of stochastic confinement is apparent: (i) The curves $\sigma(\tau_d)$ tend to peak around $\tau_d\sim\tau_c$ for large noisy modulations [Fig. 8(a)] and/or short correlation times [Fig. 8(b)]. (ii) The asymmetric confinement becomes more effective on increasing Q_1,Q_2 for $\tau_d\sim\tau_c$. Here we limit ourselves to a qualitative interpretation of these observations: When the relative time lag of ϵ_1,ϵ_2 grows much larger than τ_c, the two signal become effectively uncorrelated and therefore incapable of trapping the particle in either well—i.e., $\sigma(\tau_d)\to 0$ for $\tau_d\to\infty$; however, as the escaping particle takes a finite time to overcome the potential barrier, a nonvanishing delay τ_d with $\tau_d<\tau_c^*$ makes the confinement mechanism, already described for the ac case, more efficient; hence the raising branch of $\sigma(\tau_d)$ with $\tau_d<\tau_c$.

V. CONCLUSIONS

In conclusion, the nonlinear mixing of additive and multiplicative zero-mean signals, periodic or random, alike, is capable of localizing a Brownian particle in one well of a symmetric bistable potential through a resonant mechanism of stochastic symmetry breaking, a mechanism that went unnoticed in previous work [15]. Correspondingly, preliminary evidence suggests that the Brownian motion on a symmetric substrate under appropriate modulation conditions may exibit resonant rectification [9,21]. Direct applications of the confinement techniques proposed in this article are within the reach of existing experimental technologies; a promising example is the control of the polarization state of the light emitted by a vertical-cavity-surface emitting laser [22].

[1] See, for a review, P. Hänggi, P. Talkner, and M. Borkovec, Rev. Mod. Phys. **62**, 251 (1990).
[2] L. Gammaitoni *et al.*, Rev. Mod. Phys. **70**, 223 (1998).
[3] H. Risken, *The Fokker-Planck Equation* (Springer, Berlin, 1984).
[4] A. Tonomura, Rev. Mod. Phys. **59**, 639 (1987); A. Tonomura *et al.*, Nature (London) **412**, 620 (2001).
[5] P. T. Korda, M. B. Taylor, and D. G. Grier, Phys. Rev. Lett. **89**, 128301 (2002).
[6] Y. Makhlin, G. Schön, and A. Shnirman, Rev. Mod. Phys. **73**, 357 (2001).
[7] See, e.g., *Advances in Chemical Physics*, edited by P. Gaspard and I. Berghardt (Interscience, New York, 1997), Vol. 101.
[8] M. Borromeo and F. Marchesoni, Europhys. Lett. **68**, 783 (2004).
[9] S. Savelev *et al.*, Europhys. Lett. **67**, 179 (2004).
[10] C. R. Doering and J. C. Gadoua, Phys. Rev. Lett. **69**, 2318 (1992).
[11] L. Gammaitoni, F. Marchesoni, and S. Santucci, Phys. Rev. Lett. **74**, 1052 (1995).
[12] C. Presilla, F. Marchesoni, and L. Gammaitoni, Phys. Rev. A **40**, 2105 (1989); L. Gammaitoni *et al.*, *ibid.* **40**, 2114 (1989).
[13] F. Marchesoni, F. Apostolico, and S. Santucci, Phys. Rev. E **59**, 3958 (1999).
[14] A. V. Granato and K. Lücke, in *Physical Acoustics*, edited by W. P. Mason (Academic, New York, 1966), Vol. IVA, p. 225; J. P. Hirth and J. Lothe, *Theory of Dislocations* (Wiley, New York, 1982).
[15] M. Löcher *et al.*, Phys. Rev. E **62**, 317 (2000); L. Gammaitoni *et al.*, Phys. Rev. Lett. **82**, 4574 (1999).
[16] M. Marchi *et al.*, Phys. Rev. E **54**, 3479 (1996).
[17] F. Marchesoni, Phys. Lett. A **119**, 221 (1986), and references therein.
[18] A. Mielke, Phys. Rev. Lett. **84**, 818 (2000).
[19] P. Hänggi, P. Jung, and F. Marchesoni, J. Stat. Phys. **54**, 1367 (1989).
[20] C. Masoller, Phys. Rev. Lett. **88**, 034102 (2002); L. S. Tsimring and A. Pikovsky, *ibid.* **87**, 250602 (2001).
[21] S. Savelev, F. Marchesoni, P. Hänggi, and F. Nori, Phys. Rev. E **70**, 066109 (2004).
[22] G. Giacomelli, *et al.*, Opt. Commun. **146**, 136 (1998); M. B. Willemsen *et al.*, Phys. Rev. Lett. **82**, 4815 (1999).